

## Supplementary Information

### Ultrafine Platinum Nanoparticles Anchored in Porous Aromatic Frameworks for Efficient Hydrogen Evolution Reaction

Shulin Li<sup>†</sup>, Yang Xiao<sup>†</sup>, Han Yan, Yuting Yang, Yuyang Tian, Xiaofei Jing<sup>\*</sup>, and Guangshan Zhu<sup>\*</sup>

*Key Laboratory of Polyoxometalate and Reticular Material Chemistry of Ministry of Education, Northeast Normal University, Changchun 130024, China*

\* Corresponding Author, [jingxf100@nenu.edu.cn](mailto:jingxf100@nenu.edu.cn) (X. Jing)  
[zhugs@nenu.edu.cn](mailto:zhugs@nenu.edu.cn) (G. Zhu)

<sup>†</sup> These authors contributed equally to this work.

## Experimental Section

### Chemicals

All chemicals and solvents were purchased from commercial suppliers without further purification. *n*-Butyllithium (2.5 M in *n*-hexane), 2-bromopyridine, PPhCl<sub>2</sub>,  $\alpha,\alpha'$ -dibromo-*p*-xylene (DB*p*X) and K<sub>2</sub>PtCl<sub>4</sub> were purchased from Alfa Aesar. Pt/C (20 wt%) was purchased from Innochem. Nickel foam (NF) was purchased Jilin Tianxuan Economic and Trade Co. Ltd. Ultra-dry 1,2-dichloroethane (DCE) was purchased from Acros Organics. Other solvents and chemicals were purchased from local commercial suppliers. Deionized water produced in the lab was used in all performed experiments.

### Characterizations

Fourier transform infrared spectroscopy (FTIR) spectra (film) were measured using a Nicolet Magna 560IR spectrometer. Solid-state <sup>13</sup>C and <sup>31</sup>P cross polarization magic angle spinning nuclear magnetic resonance (CP/MAS NMR) measurements were performed on a Bruker Avance III model 400 MHz NMR spectrometer at a MAS rate of 5 kHz. Scanning electron microscopy (SEM) imaging was performed on a JEOS JSM 6700. Transmission electron microscopy (TEM) was recorded using a JEOL JEM 3010 with an acceleration voltage of 300 kV. Inductively coupled plasma atomic emission spectrometer (ICP-AES) was measured by LEEMAN Prodigy. X-ray photoelectron spectroscopy (XPS) was performed using a Thermo ESCALAB 250. Thermogravimetric analysis (TGA) was performed using a Perkin-Elmer TGA analyzer system at a heating rate of 10 °C min<sup>-1</sup> in air. Powder X-ray diffraction (PXRD) was performed with a Siemens D5005 diffractometer with scanning rate of 5 °C min<sup>-1</sup> (2 $\theta$ ). The gas adsorption-desorption isotherms were measured on a Quantachrome Autosorb-iQ2 analyzer.

### Synthesis of bis(2-pyridyl)phenylphosphine (PhPy<sub>2</sub>P)

2-Bromopyridine (40 mmol) in 25 mL of anhydrous ethyl ether was added dropwise into 16 mL of *n*-butyllithium (2.5 M in *n*-hexane) at -70 °C under vigorous stirring for 15 min. The resulting reddish-brown solution was diluted with 10 mL ultra-dry ethyl ether and stirred for another 4 h. PPhCl<sub>2</sub> (40 mmol) in 10 mL ultra-dry ethyl ether and an additional 20 mL ethyl ether were added into the above mixture. The resulting orange-brown suspension was stirred vigorously at 70 °C for 2 h and then warmed up to room temperature. The mixture was extracted with 50 mL of sulfuric acid (2 M). After that, saturated NaOH aqueous solution was introduced to adjust the pH value to 8-9. The yellow solid was collected by filtration and then washed with water and petroleum ether. The

product was purified by recrystallization with acetone/petroleum ether (yields for 50%).<sup>1</sup>

### Synthesis of Pt-PhPy<sub>2</sub>P

PhPy<sub>2</sub>P (1 mmol) was firstly dissolved in methanol/dichloromethane (V : V = 1 : 1.5) solution. Then K<sub>2</sub>PtCl<sub>4</sub> (1 mmol) aqueous solution was added into the above mixture and stirred for 24 h. The yellow product was filtered and washed with ether and *n*-hexane repeatedly, and then dried under vacuum at 80 °C for 12 h with yields of 60%.

### Synthesis of PAF-99 and Pt-PAF-99

As for PAF-99, PhPy<sub>2</sub>P (1 mmol), DBpX (2 mmol) and FeCl<sub>3</sub> (8 mmol) were added into a 100 mL two-neck flask equipped with a condenser. Degassing with three freeze-pump-thaw cycles were then used to ensure the reaction system under a N<sub>2</sub> atmosphere. After that, 20 mL of ultra-dry DCE solvent was injected into the reaction system. The mixture was stirred at 45 °C for 12 h and then heated to 80 °C and stirred for 48 h. When the reaction completed, 50 mL of methanol was poured into the mixture and the precipitate was collected by filtration. Pt-PAF-99 was synthesized following the above procedure with the monomer Pt-PhPy<sub>2</sub>P. The resulting materials were thoroughly washed with water, tetrahydrofuran, methanol and dichloromethane to remove the unreacted monomers and catalysts, and then dried at 60 °C for 12 h under vacuum to obtain brown powders with yields about 80%.

### Preparation of Pt@PAF-99

In a general process, 25 mg of PAF-99 was dispersed in 50 mL of methanol, and then 1 mL of K<sub>2</sub>PtCl<sub>4</sub> aqueous solution (10 mg mL<sup>-1</sup>) was added to the mixture under ultrasonic dispersion for 5 min. Subsequently, the reaction mixture was heated at 65 °C for 5 h. The brown product was filtered and washed three times with ethanol/acetone (V : V = 1 : 8) and dried at 60 °C under vacuum.<sup>2</sup>

### Electrochemical Measurements

The ink for working electrode was prepared by mixing ethanol (0.45 mL), Nafion solution (0.05 mL, 5 wt%), PAF catalyst (7 mg) and VULCAN XC-72 (3 mg) well under ultrasonic dispersion for 30 min. Then, 80 μL of the ink was uniformly loaded onto a clean NF (1\*0.8 cm<sup>2</sup>) as the working electrode with a catalyst loading of 1.4 mg cm<sup>-2</sup>. All electrochemical characterizations were performed in a three-electrode cell using a CHI 760E electrochemical workstation (Shanghai Chenhua Instrument Co. Ltd.). A carbon rod was used as the counter electrode in alkaline solution, and Ag/AgCl (3.5 M KCl) was applied as the reference electrode. All the measured potentials were converted to RHE:  $E_{\text{RHE}} = E_{\text{Ag/AgCl}} + 0.059 \times \text{pH} + E^{\circ}_{\text{Ag/AgCl}}$ . All the measurements were carried out in 1 M KOH solution

(pH =13.8) after purging with N<sub>2</sub> gas for 30 min at room temperature. Linear sweep voltammograms (LSVs) were obtained from 0 to 0.5 V vs RHE at a sweep rate of 5 mV s<sup>-1</sup> and corrected with 95% *iR*-compensation. Cyclic voltammetry (CV) was recorded in the non-Faradaic region between -1.1 and -1.2 V vs RHE with an increasing scan rate of 25, 50, 75, 100 and 125 mV s<sup>-1</sup>, respectively for the double-layer capacitance (*C<sub>dl</sub>*) measurements. The *C<sub>dl</sub>* can be further converted into ECSA using the specific capacitance value for a flat surface of the sample (estimated to be 0.04 mF cm<sup>-2</sup>), and ASA is the actual

surface area of the electrode, according to 
$$ECSA = \frac{C_{dl}}{C_s} \times ASA$$
. Electrochemical impedance spectroscopy (EIS) was carried out at -1.2 V vs RHE over a frequency range from 100 kHz to 0.1 Hz with a 5 mV AC dither. The chronoamperometry measurement was conducted for 43200 s under the overpotential of 10 mA cm<sup>-2</sup>.

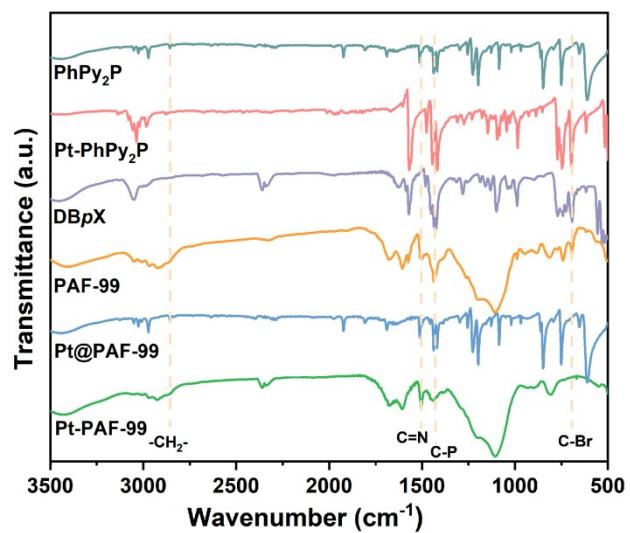


**Fig. S1** FTIR spectra of PAF-99, Pt@PAF-99, Pt-PAF-99, and their corresponding monomers, respectively.

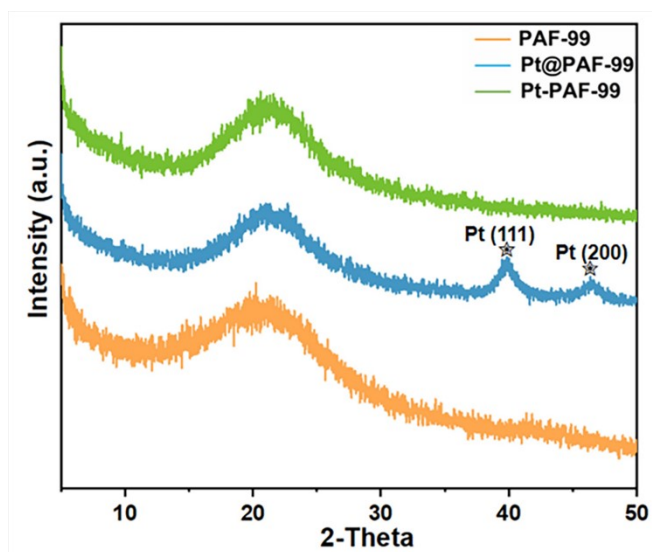


**Fig. S2** PXRD patterns of PAF-99, Pt@PAF-99 and Pt-PAF-99, respectively.

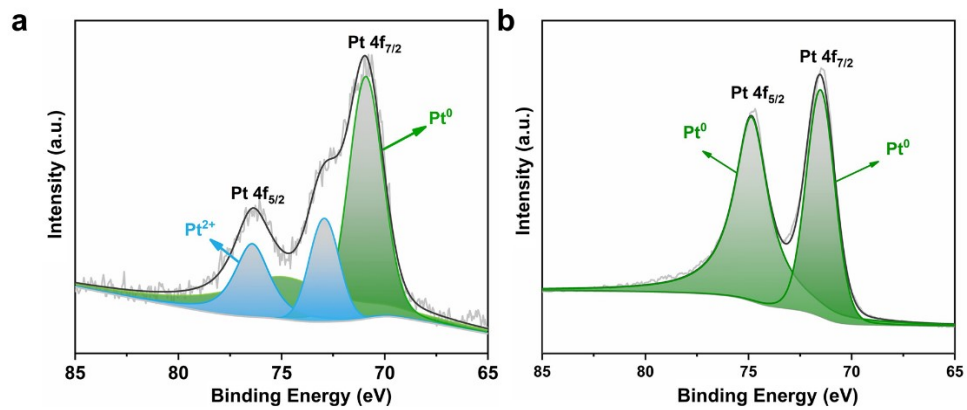


**Fig. S3** XPS spectra of Pt 4f for Pt-PAF-99 (a) and Pt@PAF-99 (b).

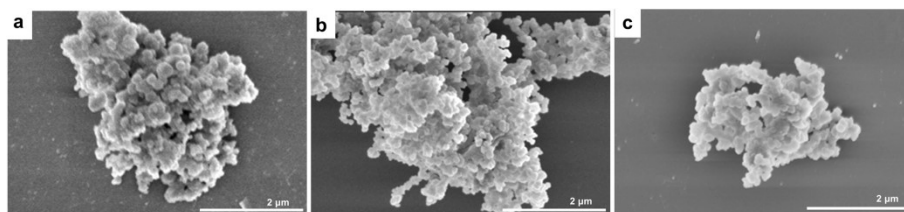


**Fig. S4** SEM images of PAF-99 (a), Pt@PAF-99 (b) and Pt-PAF-99 (c), respectively.

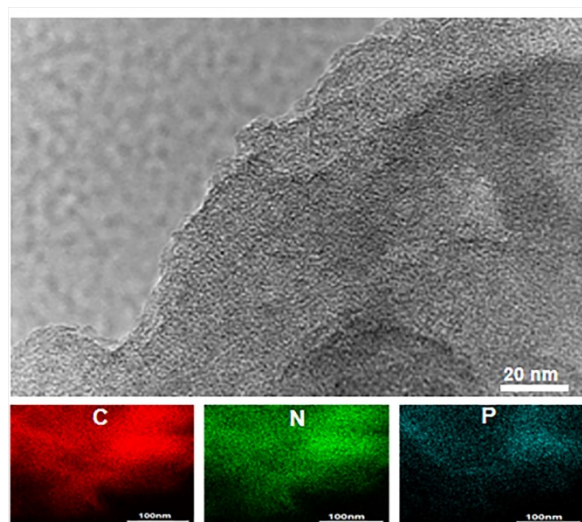


**Fig. S5** TEM image and EDX elemental mapping of PAF-99.

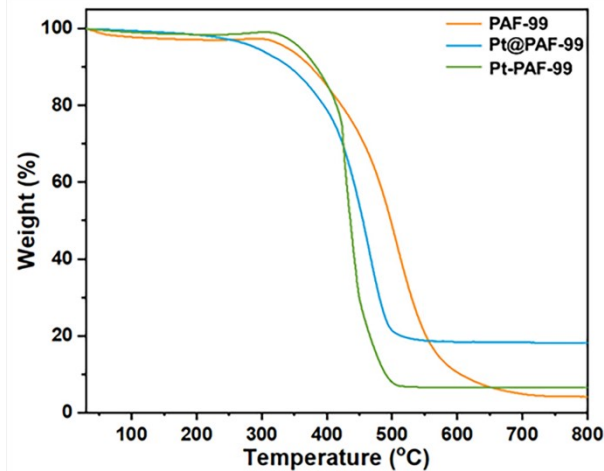


**Fig. S6** TGA curves of PAF-99, Pt@PAF-99 and Pt-PAF-99, respectively.

**Table S1** The Pt contents in Pt-PAF-99 and Pt@PAF-99 calculated from TGA and ICP analysis.

Sample	TGA (wt %)	ICP (wt %)
Pt-PAF-99	6.48	4.37
Pt@PAF-99	13.9	9.95



**Table S2** HER performances for this work and reported Pt-based HER catalysts.

	<b>Overpotential (mV) at 10 mA cm<sup>-2</sup></b>	<b>Electrolyte</b>	<b>References</b>
<b>Pt-PAF-99</b>	<b>56</b>	<b>1 M KOH</b>	<b>This Work</b>
<b>Pt@PAF-99</b>	<b>63</b>	<b>1 M KOH</b>	<b>This Work</b>
<b>Pt/OHC</b>	<b>39</b>	<b>0.5 M H<sub>2</sub>SO<sub>4</sub></b>	<b>3</b>
<b>Pt SASs/AG</b>	<b>12</b>	<b>0.5 M H<sub>2</sub>SO<sub>4</sub></b>	<b>4</b>
<b>NPCN-Pt</b>	<b>39</b>	<b>1 M KOH</b>	<b>5</b>
<b>Pt/OLC</b>	<b>38</b>	<b>0.5 M H<sub>2</sub>SO<sub>4</sub></b>	<b>6</b>
<b>Pt<sub>3</sub>Ni<sub>2</sub> NWs-S/C</b>	<b>42</b>	<b>1M KOH</b>	<b>7</b>
<b>PtNPs/CNFs</b>	<b>175</b>	<b>0.5 M H<sub>2</sub>SO<sub>4</sub></b>	<b>8</b>
<b>Pt@PCM</b>	<b>139</b>	<b>1 M KOH</b>	<b>9</b>
<b>Pt(w-Melm)</b>	<b>60</b>	<b>1 M KOH</b>	<b>10</b>

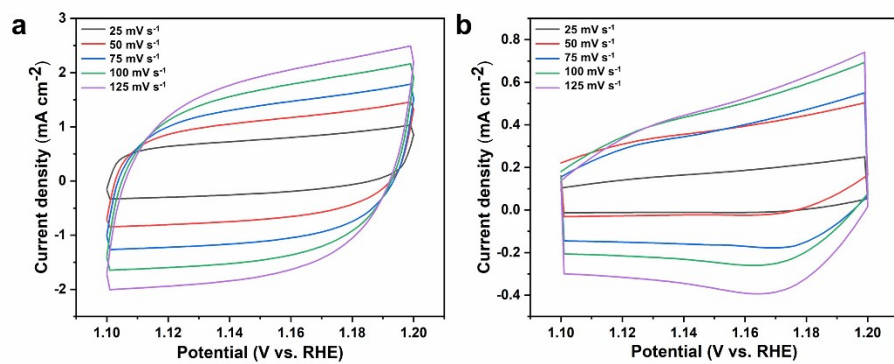


**Fig. S7** CV curves measured at different scan rates of Pt/C (a) and NF (b), respectively.

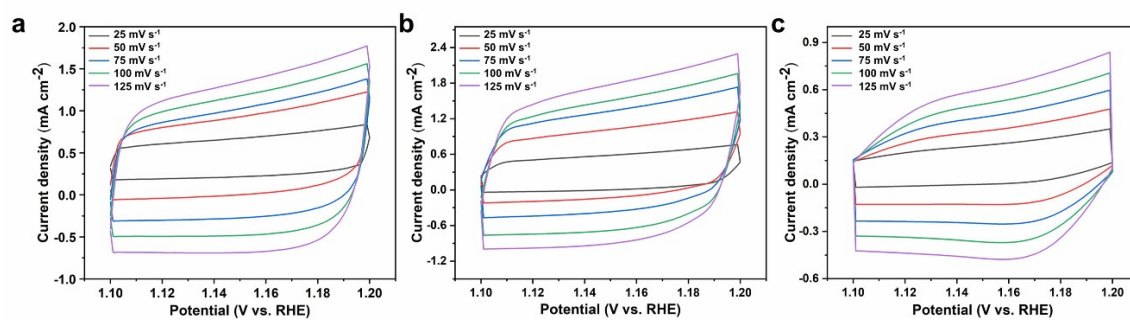


**Fig. S8** CV curves measured at different scan rates for PAF-99 (a), Pt@PAF-99 (b) and Pt-PAF-99 (c), respectively.

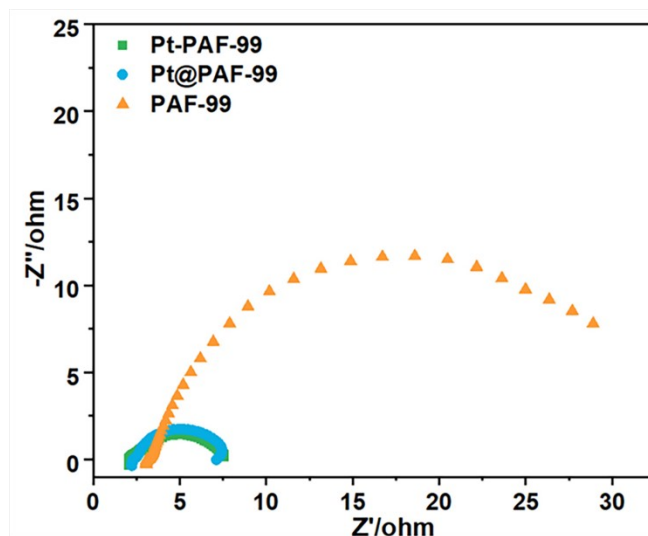


**Fig. S9** Nyquist plots of PAF-99, Pt@PAF-99 and Pt-PAF-99, respectively.

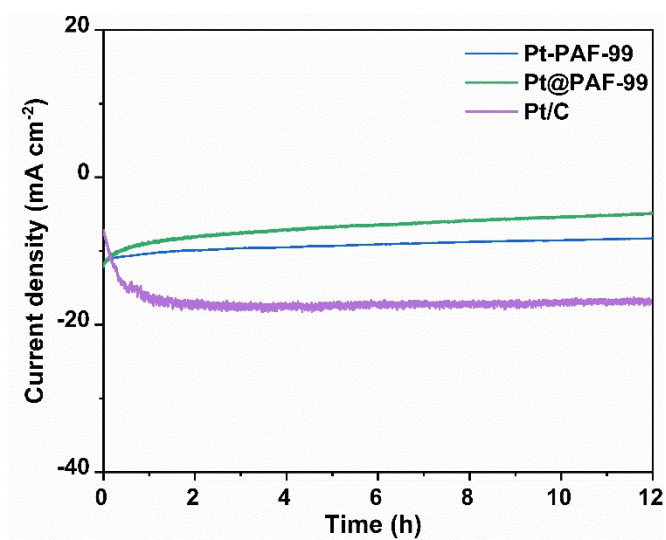


**Fig. S10** Chronoamperometry curve of Pt-PAF-99 at  $10 \text{ mA cm}^{-2}$  in 1 M KOH.

## Reference

- 1 S. A. Saucedo Anaya, A. Hagenbach and U. Abram, *Polyhedron*, 2008, **27**, 3587-3592.
- 2 Y. Yang, T. Wang, X. Jing and G. Zhu, *J. Mater. Chem. A*, 2019, **7**, 10004-10009.
- 3 Z. Wang, Y. Yang, J. Mo, C. Zhao and C. Yan, *Colloid Surface A*, 2023, **656**, 392-399.
- 4 S. Ye, F. Luo, Q. Zhang, P. Zhang, T. Xu, Q. Wang, D. He, L. Guo, Y. Zhang, C. He, X. Ouyang, M. Gu, J. Liu and X. Sun, *Energy Environ. Sci.*, 2019, **12**, 1000-1007.
- 5 C. Wang, F. Chen, Q. Wang, X. Yang, H. Zang, N. Yu and B. Geng, *Carbon*, 2023, **201**, 278-284.
- 6 D. Liu, X. Li, S. Chen, H. Yan, C. Wang, C. Wu, Y. A. Haleem, S. Duan, J. Lu, B. Ge, P. M. Ajayan, Y. Luo, J. Jiang and L. Song, *Nat. Energy*, 2019, **4**, 512-518.
- 7 P. Wang, X. Zhang, J. Zhang, S. Wan, S. Guo, G. Lu, J. Yao and X. Huang, *Nat. Commun.*, 2017, **8**, 580-588.
- 8 T. Yang, M. Du, H. Zhu, M. Zhang and M. Zou, *Electrochim. Acta*, 2015, **167**, 48-54.
- 9 H. Zhang, P. An, W. Zhou, B. Guan, P. Zhang, J. Dong, X. Lou, *Sci. Adv.*, 2018, **4**, 57-65.
- 10 Z. N. Zahran, E. A. Mohamed, T. Katsuki, Y. Tsubonouchi, D. Chandra, N. Hoshino and M. Yagi, *Sustain. Energ. Fuels*, 2022, **6**, 4265-4274.